

1 **ADM1 modelling of large-scale covered in-ground anaerobic reactor treating sugarcane**
2 **vinasse**

3 Marcelo Leite Conde Elaiuy^{a*}, Aiduan Li Borrion^b, Davide Poggio^c, Julia Anna Stegemann^d, Edson
4 Aparecido Abdul Nour^e

5 ^a *University College London, Department of Civil, Environmental & Geomatic Engineering, Centre*
6 *for Resource Efficiency & the Environment (CREE), Chadwick Building, Gower Street, London*
7 *WC1E 6BT, United Kingdom – m.elaiuy@ucl.ac.uk*

8 ^b *University College London, Department of Civil, Environmental & Geomatic Engineering, Centre*
9 *for Resource Efficiency & the Environment (CREE), Chadwick Building, Gower Street, London*
10 *WC1E 6BT, United Kingdom – a.borrion@ucl.ac.uk*

11 ^c *Energy 2050, Department of Mechanical Engineering, Faculty of Engineering, University of*
12 *Sheffield, Sheffield S10 2TN, UK – d.poggio@sheffield.ac.uk*

13 ^d *University College London, Department of Civil, Environmental & Geomatic Engineering, Centre*
14 *for Resource Efficiency & the Environment (CREE), Chadwick Building, Gower Street, London*
15 *WC1E 6BT, United Kingdom – j.stegemann@ucl.ac.uk*

16 ^e *University of Campinas, School of Civil Engineering, Architecture and Urban Design, Saturnino*
17 *de Brito, 224, Cidade Universitária Zeferino Vaz, Campinas SP, 13083-889, Brazil –*
18 *ednour@fec.unicamp.br*

19

20

21

22

* Corresponding author: m.elaiuy@ucl.ac.uk (M.L.C. Elaiuy)

23 **ABSTRACT**

24 In this paper, we demonstrate in a clear procedure the application of ADM1 to model a large-scale
25 covered in-ground anaerobic reactor (Cigar), processing sugarcane vinasse from a biorefinery in
26 Brazil. The biochemical make-up (carbohydrates, proteins, and lipids) of the substrate was analysed
27 based on the food industry standards. Two distinct subsets of data, based on the sugarcane harvest
28 season for bioethanol and sugar production in 2012 and 2014, were used to direct and cross validate
29 the model, respectively. We fitted measured data by estimating two key parameters against biogas
30 flow rate: the degradation extent (f_d) and the first order hydrolysis rate coefficient (k_{hyd}). By cross-
31 validation we show that the fitted model can be generalised to represent the behaviour of the reactor
32 under study. Therefore, motivated by practical and industrial application of ADM1, for both
33 different reactors types and substrates, we show aspects on the implementation of ADM1 to a
34 specific large-scale reactor for anaerobic digestion of sugarcane vinasse.

35 **Keywords** ADM1, anaerobic digestion, biogas; simulation, sugarcane vinasse

36 **INTRODUCTION**

37 Sugarcane bioethanol has been produced in many countries/regions, such as Brazil, the USA and
38 the European Union and is regarded as one of the most promising alternatives to replace fossil fuels.
39 However, such interest has led to bioethanol expansion and the saying “what goes in must come
40 out”, is especially true for the sugar-bioethanol industry, which produces huge amounts of residues,
41 including sugarcane vinasse (SV), a dark brown wastewater after bioethanol distillation. The
42 projections by the Agricultural Trade Office (ATO/São Paulo) of total bioethanol production in
43 Brazil’s marketing year (MY) 2017/18 were 26.65 billion litres (11.83 billion litres of anhydrous
44 bioethanol and 14.82 billion litres of hydrated bioethanol) (GAIN 2017). On average Brazilian
45 biorefineries produce 12 L of SV for each litre of bioethanol. The trade-off between the
46 concentration of alcohol and the viability of yeast limits the reduction of SV volumes.
47 SV has been extensively worldwide used as fertilizer in the sugarcane fields given the presence of
48 rich minerals, such as potassium, calcium, magnesium, phosphorus, and nitrogen. SV can also be

49 applied onto so-called “sacrifice areas” in Brazil when not used as fertilizer. However, in both
50 cases there is a great risk of environmental contamination. The emission and degradation of SV in
51 the terrestrial and aquatic environment can cause severe impacts, such as eutrophication of rivers
52 and lakes, ground water contamination and GHG (greenhouse gas) emissions (Moraes et al. 2015).
53 Nevertheless, effective and economic biological treatment of SV, such as anaerobic digestion (AD)
54 has been often cited as an option for mitigating the environmental impacts (Leite et al. 2015,
55 Moraes et al. 2015).

56 AD arises as a sustainable bioprocess to unlock the value of SV as an energy feedstock. It is a
57 biological engineering solution that improves the attractiveness of bioethanol as an alternative fuel,
58 both as a means of pollution potential reduction and through recovery of biogas for renewable
59 bioenergy generation (Barrera et al. 2015, Leite et al. 2015). Moreover, biogas produced by AD can
60 replace the burning of bagasse, which is a by-product from the first-generation bioethanol
61 production, to encourage second-generation bioethanol production from bagasse (Moraes et al.
62 2015). However, the industrial exploitation of SV has been hampered by inefficient reactors and/or
63 their improper operation. An experimental approach coupled with mathematical models can support
64 optimisation of a biological system and the prediction of reactor behaviour/efficiency under
65 different conditions (Donoso-Bravo et al. 2011). Nevertheless, the industrial application of models
66 is not widespread given the diversity and specific nature of most industrial processes (Batstone &
67 Keller 2003). In addition, the complexity and non-linearity of the AD process and the considerable
68 demand of experimental data for modelling purposes are barriers to modelling at industrial scale.

69 To date, the Anaerobic Digestion Model No. 1 (ADM1) (Batstone et al. 2002) is commonly
70 regarded as the most realistic and generic model to describe the main biochemical and physico-
71 chemical processes, and gas-liquid mass transfer in anaerobic digestion (Poggio et al. 2016).
72 According to Batstone et al. (2006), ADM1 was originally developed: 1) for full-scale application
73 in plant design, operation, and optimisation, 2) as a working platform for model improvement
74 based on validation studies, and 3) to fulfil the industry needs as a technology transfer tool,

75 developing operational strategies and evaluating the performance of controllers (Batstone & Steyer
76 2007). Although the ADM1 Scientific Technical Report (STR) states that the model was developed
77 for application in industry (Batstone et al. 2006), its industrial use to describe a large-scale covered
78 in-ground anaerobic reactor (Cigar) to process wastewater from sugarcane biorefinery has not been
79 reported in the literature. In addition, the practical application of ADM1 under real operating
80 conditions is a difficult task, and the modelling framework presented here addresses some of the
81 issues generating substantial information assessing the viability of model application using real
82 plant data.

83 The research reported in this paper applies ADM1 in a clear procedure to model the first large-scale
84 Cigar in Brazil, which processes SV to produce biogas and generate bioelectricity for supply to the
85 local grid. The Cigar is one of the components integrating a full biogas plant.

86 Good modelling practice requires both direct and cross validation and to this end a reasonable
87 volume of data must be available and divided into two subsets. Direct validation consists in
88 evaluating the ability of the model to reproduce the experimental data used for estimating the
89 parameters. It is a necessary condition but not enough to accept the ability of the model to
90 reproduce the behaviour of the system under study. In fact, even fitting well the data used for
91 parameter estimation, the model may not be generalized to represent the behaviour of the system
92 under study by using another subset. Therefore, in this work two subsets of data, based on the
93 sugarcane harvest season for bioethanol and sugar production in 2012 and 2014, were used to direct
94 and cross validate the model, respectively.

95 **METHODS**

96 **Cigar set-up and operation**

97 The modelled large-scale anaerobic methanogenic reactor for digestion of SV, Cigar, is located in
98 the area of Ester Mill in the city of Cosmópolis, South East, Brazil. It was designed based on
99 historical qualitative and quantitative data for SV produced by Ester mill, and its design
100 characteristics are shown in Table 1. In the study periods presented here of 2012 (from May 2012 to

101 December 2012) and 2014 (from August 2014 to November 2014), the Ester Mill sugar production
 102 was 110,400 and 100,200 tonnes, respectively. Within the same periods, the hydrous bioethanol
 103 production was 69 million and 62 million litres, respectively.

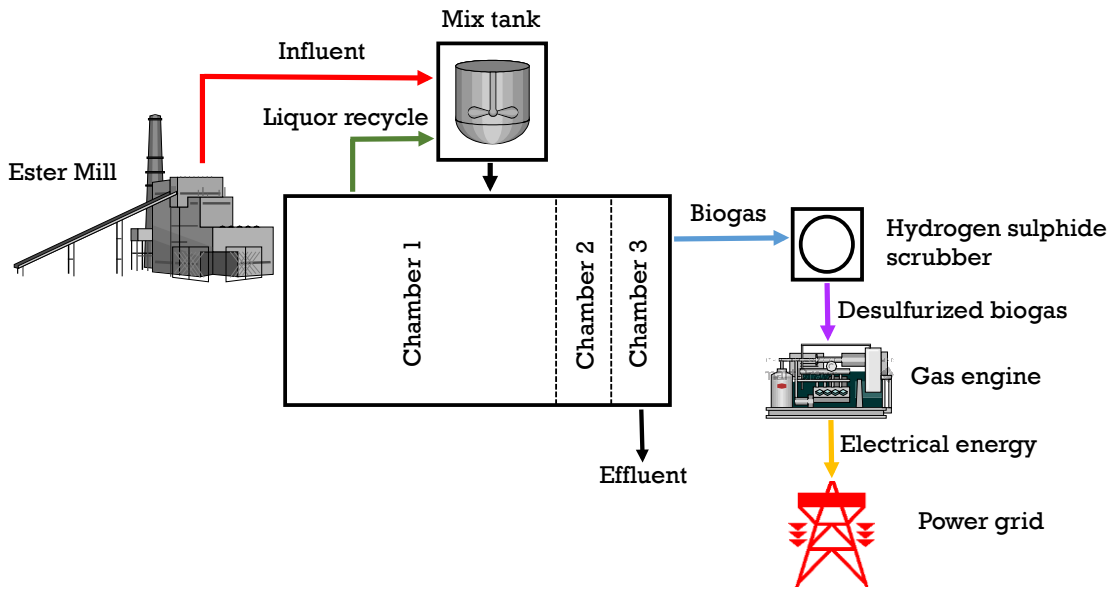
104 Table 1. Cigar design parameters and main operational data.

Parameter	Value	Units
Flow rate of SV	39.5	m ³ h ⁻¹
Concentration of organic matter	30	kg COD m ⁻³
Organic Loading Rate (OLR)	1.99	kg COD m ⁻³ day ⁻¹
Reactor volume	15,000	m ³
Headspace volume	4,800	m ³
Hydraulic Retention Time	15	days
Conversion rate	0.228	m ³ CH ₄ kg COD ⁻¹
Biogas rate production	491	Nm ³ h ⁻¹
Methane rate production (55%)	270	N m ³ h ⁻¹ CH ₄

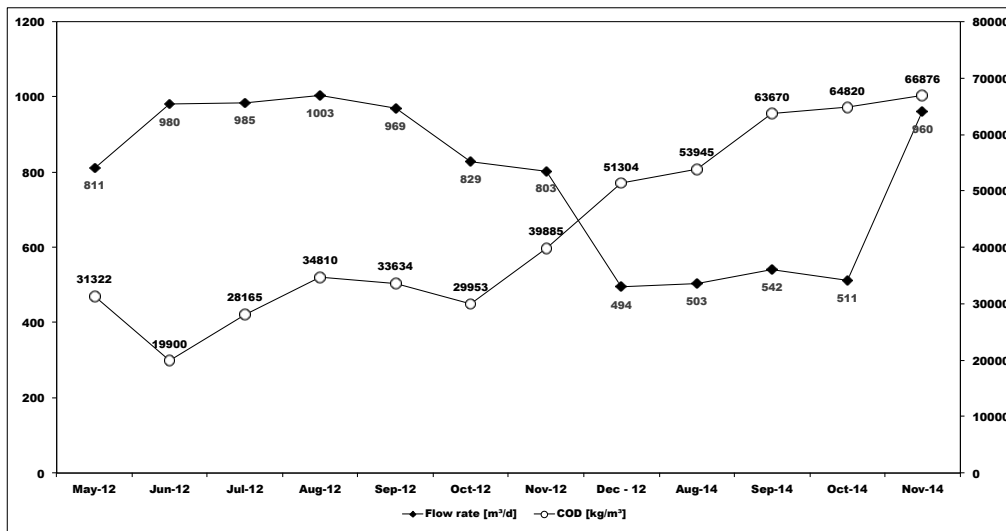
105 The reactor is operated under mesophilic conditions at approximately 37°C. The average hydraulic
 106 retention time (HRT) was 15 days and Cigar was inoculated with sludge from industrial and
 107 domestic sewage treatment plants for the first time in 2010. The blanket of microorganisms in the
 108 reactor reached maturity after one and a half years (i.e., steady-state).

109 Figure 1 presents a simplified schematic flow diagram for Cigar and the other components (mix
 110 tank, hydrogen sulphide scrubber, and gas engine) of the biogas plant. Cigar is a 3-chamber reactor
 111 where chamber 1 and 2, represent 60% and 20% of total reactor volume, respectively. The
 112 remaining 20% volume of chamber 3 is responsible for settling most of the biological activated
 113 sludge. The SV from the biorefinery is mixed with liquor from chamber 1 to recirculate the
 114 alkalinity, with effect of an overall rise in the influent pH. This mixture enters Cigar from the
 115 bottom and flows upwards, as in a typical upflow anaerobic sludge blanket (UASB) reactor, without
 116 the phase separator at the top, providing favourable physical and chemical conditions for sludge
 117 flocculation. An automated pumping station adjusts flow rates in Cigar, which was measured online
 118 using an electromagnetic flow meter model OPTIFLUX KC1000F/6 (Krohne) with a signal
 119 converter IFC 100. The flow rate was adjusted based on the organic loading in the SV. Over the
 120 study periods, in 2012 and 2014, there were significant variations in the COD concentration and
 121 flow rate as can be observed in Figure 2.

122 The biogas produced is drawn from the reactor headspace and transferred to an aerobic biological
 123 scrubbing system for removal hydrogen sulphide. The biogas is then burned in a gas engine
 124 connected to a 1 MWe containerized power generation set to produce bioelectricity feeding the
 125 local energy grid.



126
 127 Figure 1. Simplified biogas plant-wide layout under study.



128
 129 Figure 2. Averages of COD concentrations and flow rate in 2012 and 2014.

130 **Cigar monitoring**

131 **Influent and effluent**

132 The mixed influent from the mix tank and the effluent from chamber 3 were sampled, analysed, and
 133 recorded based on the biogas plant operating routine, containing the most relevant information at
 134 the lowest cost of monitoring. Since the reactor was located in a remote area, the biogas plant

135 counted on a laboratory scale to carry out same day analyses to avoid either sample storage or
 136 transport. Recorded data from online and offline analyses provided by the plant operators were used
 137 in the model simulations. The sample collection and physico-chemical analyses of the mixed
 138 influent in the mix tank and the effluent in chamber 3, were done frequently by plant operators
 139 according to the protocols described by the Standard Methods for the Examination of Water and
 140 Wastewater (APHA 2012) – Table 2.

141 Table 2. Physico-chemical parameters analysed, method and frequency.

Parameter	(APHA, 2012)	Frequency
Temperature	2550	constant (online)
pH	4500	constant (online)
COD concentration	5220	daily (offline)
Total solids (TS)	2540B	weekly (offline)
Total volatile solids (TVS)	2540E	weekly (offline)
Total suspended solids (TSS)	2540D	weekly (offline)
Volatile suspended solids (VSS)	2540E	daily (offline)
Volatile fatty acids (VFA)	5560	daily (offline)
Partial alkalinity	2320	daily (offline)
Total Kjeldahl nitrogen (TKN)	4500	fortnightly (offline)
Total ammonia nitrogen (TAN)	4500	fortnightly (offline)

142 The biochemical composition of the substrate was divided amongst, carbohydrates, lipids and
 143 proteins, and analyzed according to the following analytical methods: carbohydrates by the Lane &
 144 Eynon (1923) method and lipids by the Bligh & Dyer (1959) method. The total protein content was
 145 estimated by multiplying the total Kjeldahl nitrogen by factor 6.25, based on the food industry
 146 standard for protein determination (Mariotti et al. 2008). The inert fraction in the influent was
 147 calculated as ash content (i.e., the difference between the average of TS and VS).

148 **Biogas**

149 The biogas flow was measured online using a Vortex M84 flow meter (Foxboro®) and its content
 150 (%CH₄) was measured using a Landtec GEM™ 2000. Equipment calibrations were undertaken
 151 constantly to ensure accuracy in the measurements.

152 **Modelling methods**

153 **Cigar implementation and inputs**

154 Cigar was implemented as a single stage model in Aquasim 2.1 d (Reichert 1998) and modelled as a
155 mixed liquid reactor with constant volume, and gas diffusion to a mixed gas headspace. For model
156 simplicity and simulation efficiency the three chambers in the Cigar were lumped together and
157 modelled as a CSTR reactor. In fact, samples at different points (chamber 1, recycle point, and
158 chamber 3) were analysed for COD, TSS, and VSS (results not shown); the results were comparable
159 in their values and showed a certain degree of sludge dispersion in the reaction zone. For this main
160 reason we believe that our reactor should be modelled as a CSTR. Reactors such as UASBs can
161 behave as CSTR, given their hydrodynamics influenced by the fluid flow characteristics, particles
162 sizes, multiphase interactions, chaotic advection, and substrate dispersion (Heertjes & Kuijnhoven
163 1982, Peña et al. 2006).

164 The original ADM1 as described in the IWA STR (Batstone et al. 2002) was used in this paper.
165 Different researchers have developed and proposed a series of extensions to functionally upgrade
166 the ADM1 to allow for plant-wide phosphorus (P) simulation (Flores-Alsina et al. 2016, Solon
167 2017) and the influence of ionic strength (as activity corrections) and ion pairing (Solon et al.
168 2015). However, those updates were not implemented in this study, given the lack of P
169 measurements in the available experimental data and the relative low ionic strength of the SV.
170 Regarding the latter, Solon et al. (2015) recommends to implement the correction for ADM1 in case
171 of high ionic strength (e.g. $I > 0.2 \text{ mol L}^{-1}$) such as in manure and high-solids digestion.
172 Likewise, different inhibition parameters and functions, compared to the original ADM1
173 implementation have been recommended, for instance, for ammonia (Wett et al. 2014, Wilson et al.
174 2012) and VFA (Pratt et al. 2012). Especially regarding ammonia, there are experimental evidences
175 that free ammonia inhibition coefficients are higher than previously believed (Batstone et al. 2010).
176 However, given the lack of consensus in the scientific community, the original implementation was
177 maintained in our study.

178 Stoichiometric and kinetic parameters were based on the work of Rosén & Jeppsson (2006). The
179 ADM1 composite material X_c , which describes the substrate, was discarded as suggested in Poggio

180 et al. (2016), avoiding a two-step solubilisation processes; instead the substrate was described
181 directly in terms of its carbohydrates, proteins, lipids and inerts fraction. The ash fraction was
182 included in the loadings to predict the accumulation of the non-biodegradable fraction of the
183 substrate in the Cigar. TS, VS measurements and the calculated ash fraction were read into
184 Aquasim as real list variables.
185 Initial conditions were established by running a whole year steady-state simulation of the same
186 system, and considering a constant loading rate equal to the average of the measured loading rates
187 of 2012 and a constant substrate composition equal to the average of the measured compositions of
188 2012 - the outputs of that simulation were used as initial conditions for the simulations here
189 presented and kept the same in the two data sets.
190 The temperature was set to 310 K (37° C) based on average historical mesophilic conditions
191 measured for Cigar. Real list variables were read into Aquasim for daily COD measurements and
192 daily feed flow rates, which were highly variable over the Cigar operation.

193 **Substrate fractionation**

194 The fractionation of the substrate into three biochemical compound groups: carbohydrates, proteins,
195 and lipids is a critical step for appropriate ADM1 implementation (Ramirez et al. 2009a). ADM1 is
196 COD-based to describe the organic matter transformations. Therefore, the elemental formula of
197 each biochemical compound, which allocates the calculated theoretical oxygen demand (ThOD),
198 was used to obtain concentrations in kgCOD m⁻³. The proportions of individual organic fractions
199 (i.e., carbohydrates, proteins, and lipids in kg m⁻³) were multiplied by the ThOD of each compound.

200 **Charge balance**

201 The charge balance was included for the description of the substrate loadings. The following
202 dynamic state variables in ADM1, S_{ac} , S_{pro} , S_{bu} , S_{va} , S_{in} , and S_{ic} have a charge, whilst all other
203 variables are electro-neutral (Nopens et al. 2009). One of the approaches for modelling acid-base
204 equations is the charge balance, described by Eq. (1) for anaerobic digestion. The unknown
205 variables are S_{CAT} , S_{AN} , and pH, with two degrees of freedom. In our case, the pH values of the

206 influent stream were used (setting α -values, OH^- , and H^+) to remove a degree of freedom. The other
207 degree of freedom was removed when S_{CAT} exceeded S_{AN} , then S_{AN} was set to zero and vice versa to
208 close the charge balance (Poggio et al. 2016).

$$209 \quad S_{\text{CAT}} - S_{\text{AN}} = S_{ac}\alpha_{ac} + S_{pro}\alpha_{pro} + S_{bu}\alpha_{bu} + S_{va}\alpha_{va} + S_{IN}\alpha_{IN} + S_{IC}\alpha_{IC} + \text{OH}^- + \text{H}^+ \quad (1)$$

210 Only total VFA was routinely analysed by plant operators and most VFA in SV was assumed to be
211 mostly acetate, as shown in Leite et al. (2015). Inorganic carbon S_{IC} , calculated through partial
212 alkalinity measurements (real alkalinity for anaerobic reactors $5.75 < \text{pH} < 8$) was set to zero, as
213 the pH of the influent was always below 5. The TAN measured in the substrate was entered as S_{IN}
214 (inorganic nitrogen fraction). The specific charge coefficient α_i was calculated as described in
215 Nopens et al. (2009). The hydrogen and hydroxide ions were determined as $\text{H}^+ = 10^{-\text{pH}}$ and $\text{OH}^- =$
216 $10^{(-\text{pK}_w + \text{pH})}$ ($\text{pK}_w = 14$).

217 The dynamic state variables changed according to feed streams, thereby S_{CAT} and S_{AN} were
218 calculated at given dates taking into account pH, VFA, inorganic nitrogen, inorganic carbon, and
219 accurate temperature measurement in the laboratory. Inputs for S_{CAT} and S_{AN} were read into
220 Aquasim as real list variables.

221 **Kinetic fractionation**

222 The COD input of SV, as in any anaerobic digestion system of organic residues, was divided into
223 biodegradable and non-biodegradable fractions (Angelidaki & Sanders 2004). The degradation
224 extent (f_d) was introduced to describe the degradable ThOD fraction of substrate that is converted to
225 methane (Jensen et al. 2011). This degradable fraction is made up of soluble fraction f_s and a
226 particulate fraction ($1-f_s$). The non-degradable fraction ($1-f_d$) is composed essentially of an inert
227 fraction X_I . The literature shows that hydrolysis and disintegration rates originally suggested in
228 ADM1 are too high and are more likely to describe activated sludge substrate (Vavilin et al. 2008,
229 Köch et al. 2010). The disintegration step was omitted assuming direct hydrolysis of proteins (X_{pr}),
230 carbohydrates (X_{ch}), and lipids (X_{li}) (Jensen et al. 2011). The particulate components of the substrate
231 (i.e., carbohydrates, proteins, and lipids) have different hydrolysis rates (Mata-Alvarez et al. 2011).

232 However, without experimental measurements of the products of hydrolysis (sugar, aminoacids,
233 LCFA) the calibration of the three hydrolysis parameters would result in a higher uncertainty in the
234 obtained values of the parameters. Therefore, to increase the parameters identifiability, only one
235 "lumped" first order hydrolysis rate parameter is considered and calibrated. A similar approach is
236 also followed by Lübken et al. (2007), Arnell et al. (2016), Batstone et al. (2009). In addition, the
237 hydrolysis of particulate substrate, which is described as rate-limiting step in anaerobic digestion
238 (Vavilin et al. 2008), was implemented by a first order hydrolysis kinetics.

239 **Parameter estimation**

240 Preliminarily, the state at the end of the first period (2012) was assumed as the initial condition for
241 parameter estimation. Further, we estimated two key parameters used to indicate the degradable
242 COD: the degradation extent (f_d) and the first order hydrolysis rate coefficient (k_{hyd}), in attention to
243 reactor dynamic inputs (Batstone et al. 2009). Also, the choice of hydrolysis was initially based on
244 the evidence that kinetic parameters used to describe hydrolysis of carbohydrates, proteins, and
245 lipids are assumed as unrealistic values in the original ADM1 (Kazadi Mbamba et al. 2016). Both
246 parameters were estimated and validated against biogas flow rate. They were estimated by a
247 function implemented in Aquasim to minimize the sum of the squares of weighted deviations
248 between measurements and calculated model outcomes (Reichert, 1998).

$$249 \quad X^2 = \sum_{i=1}^n \left(\frac{y_{m,i} - y_i(p)}{\sigma_{m,i}} \right)^2 \quad (2)$$

250 where $y_{m,i}$ is the i^{th} measured value of the target measurement, assumed to be a normally distributed
251 random variable; $y_i(p)$ is the model prediction at the time corresponding to data point i , which could
252 be considered a function of the set of parameters p to be estimated; $\sigma_{m,i}$ is the standard error of the
253 measurement $y_{m,i}$ and weights each term of the sum.

254 The secant algorithm in Aquasim was selected for numerical minimization of Eq. (2) due to
255 possible nonlinearity of the model equations and numerical integration procedure (Lübken et al.
256 2007). The standard error of the estimated parameters are calculated by Aquasim as an output of the

257 secant algorithm, and then divided by the estimated values to determine the uncertainty in the
258 parameters. We therefore present a more reliable evidence of representing model uncertainty than
259 providing only model goodness of fit values (Jensen et al. 2011).

260 **Model validation**

261 To assess the accuracy of predictions for direct and cross validation using two subsets of data based
262 on the sugarcane harvest season in 2012 and 2014, the relative absolute error (rAE) between
263 measured and simulated values was determined as per Eq. (3), where $y_{m,i}$ is the i^{th} measured value,
264 assumed to be a normally distributed random variable; $y_i(p)$ is the model prediction at the time
265 corresponding to data point i , which could be considered a function of the set of parameters p to be
266 estimated and n is the number of observations. This allow us to classify the quality of predictions
267 according two classes (Batstone & Keller 2003): high ($\pm 10\%$) or medium (10% - 30%) accurate
268 quantitative prediction.

$$269 \quad rAE = \frac{\sum_{i=1}^n \left(\frac{|y_{m,i} - y_i(p)|}{y_{m,i}} \right)}{n} \quad (3)$$

270 **RESULTS**

271 **SV characterization and biochemical fractionation**

272 The SV feed stream for Cigar in both periods of study was characterized based on samples analysed
273 in the laboratory scale biogas plant. The average results from 2012 and 2014 are shown in Table 3.
274 Average COD and total solids in 2014 were both twice those in 2012. This can be explained
275 because the biorefinery produced more sugar than bioethanol in 2014/2015, leaving higher
276 concentrations in the SV. Also high concentration of organic matter in SV is generally followed by
277 an increase in organic acids levels, which explains about twofold of VFA in 2014 compared to
278 2012.

279

280

281 Table 3. Average substrate characterization \pm standard deviation in 2012 and 2014.

Parameter	2012	2014	Units
pH	4.03 \pm 0.4	4.04 \pm 0.2	n/a
COD concentration	30.55 \pm 11.2	61.04 \pm 7.6	g L ⁻¹
Total solids (TS)	24.06 \pm 7.8	42.22 \pm 6.3	g L ⁻¹
Total volatile solids (TVS)	17.15 \pm 7.5	32.21 \pm 4.2	g L ⁻¹
Total suspended solids (TSS)	11.4 \pm 8.4	10.18 \pm 5.2	g L ⁻¹
Volatile suspended solids (VSS)	8.22 \pm 6.3	5.54 \pm 2.1	g L ⁻¹
Volatile fatty acids (VFA)	2.36 \pm 0.8	4.02 \pm 1.4	g L ⁻¹
Partial alkalinity	0	0	gCaCO ₃ L ⁻¹
Total Kjeldahl nitrogen (TKN)	0.41 \pm 0.09	0.45 \pm 0.16	g L ⁻¹
Total ammonia nitrogen (TAN)	0.15 \pm 0.11	0.19 \pm 0.08	gN-NH ₄ L ⁻¹

282 Table 4 shows the results of the substrate biochemical fractionation in carbohydrates (f_{ch}), proteins
 283 (f_{pr}), and lipids (f_{li}) on a COD basis. The carbohydrates concentration is higher than lipids and
 284 proteins as found in Barrera et al. (2015). However, it is noteworthy that protein content of the SV
 285 analysed in this study was relatively high when compared to other studies (Leite et al. 2015, Barrera
 286 et al. 2015). In the bioethanol distillery the yeast *Saccharomyces cerevisiae* resulting from alcohol
 287 fermentation is composed by 26.95% of crude protein, which may be lost during the process to the
 288 SV. Another assumption for the high protein content is possibly the estimation using a constant
 289 factor of 6.25 as reported in Mariotti et al. (2008).

290 Table 4. Fractionation of substrate into biochemical compounds.

Biochemical compost	Concentration (g/L)	Elemental* formula	ThOD (gCOD/gVS)	Concentration (gCOD/L)	(% COD _{th})
Carbohydrates (f_{ch})	4.4	C ₆ H ₁₀ O ₅	1.184	5.21	44%
Proteins (f_{pr})	2.6	C ₅ H ₇ O ₂ N	1.415	3.68	30%
Lipids (f_{li})	1.1	C ₅₇ H ₁₀₄ O ₆	2.874	3.16	26%

291 *Angelidaki & Sanders (2004)

292 The charge balance influences directly the reactor pH and its results are shown in Table 5, indicated
 293 as state variables in ADM1. Despite the fact plant operators claimed to analyse the influent frequently,
 294 necessary data to calculate S_{CAT} and S_{AN} was only found at given dates shown in Table 5. This in turn
 295 would possibly affect the results of pH, which is an interaction of all charge bearing species in the
 296 system, and will be discussed later.

297

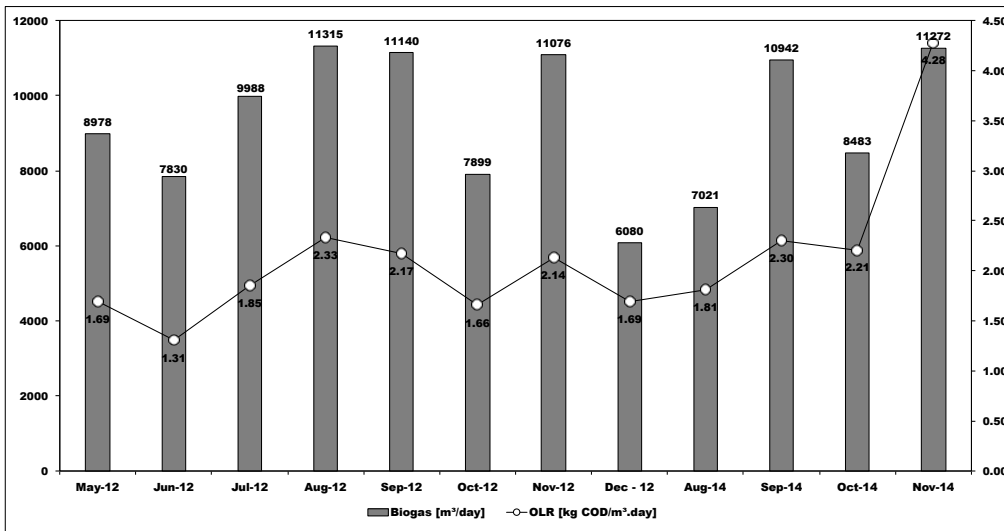
298 Table 5. Substrate description based on charge balance.

Date	pH	VFA - S_{ac} (gCOD L ⁻¹)	ADM1 state variables			
			S_{IC} (kmol m ⁻³)	S_{IN} (kmol m ⁻³)	S_{CAT} (kmol m ⁻³)	S_{AN} (kmol m ⁻³)
2012						
05/09	4.15	2.793	0	0.0117	0	0.0054
02/10	3.87	2.029	0	0.0117	0	0.0083
09/10	3.85	2.806	0	0.0122	0	0.0076
16/10	3.53	2.305	0	0.0196	0	0.0180
23/10	3.85	2.241	0	0.0086	0	0.0050
30/10	4.74	1.631	0	0.0089	0.003	0
06/11	4.09	3.525	0	0.01071	0	0.0011
14/11	4.00	2.664	0	0.0143	0	0.0083
20/11	4.17	3.563	0	0.0085	0.003	0
23/11	3.99	3.191	0	0.0173	0	0.0025
27/11	4.24	3.274	0	0.0275	0.001	0
2014						
01/08	4.12	3.807	0	0.025	0	1.67E-10
06/08	4.21	7.942	0	0.0214	0.005	2.05E-10
13/08	4.28	5.059	0	0.0277	0	2.41E-10
15/08	4.47	5.059	0	0.0286	0	3.74E-10
27/08	3.8	4.353	0	0.0338	0	7.99E-11
29/08	4.2	4.301	0	0.0344	0	2.01E-10
03/09	4.18	4.680	0	0.0339	0	1.92E-10
05/09	4.15	4.699	0	0.329	0	1.79E-10
10/09	4.03	4.179	0	0.0274	0	1.36E-10
17/09	4.21	5.322	0	0.0236	0	2.05E-10
19/09	3.84	4.051	0	0.0189	0	8.76E-11
26/09	4.19	2.343	0	0.0216	0	1.96E-10
01/10	4.21	4.693	0	0.257	0	2.05E-10
03/10	3.9	3.428	0	0.0264	0	1.01E-10
08/10	3.45	3.351	0	0.0238	0	3.57E-11

299

300 **Performance of the CIGAR**

301 Figure 3 shows a good correlation between the average organic loading and the biogas flow rate, as
 302 should be expected in a non-inhibited system. However, the biogas production tends to decline
 303 relatively to the OLR in 2014.



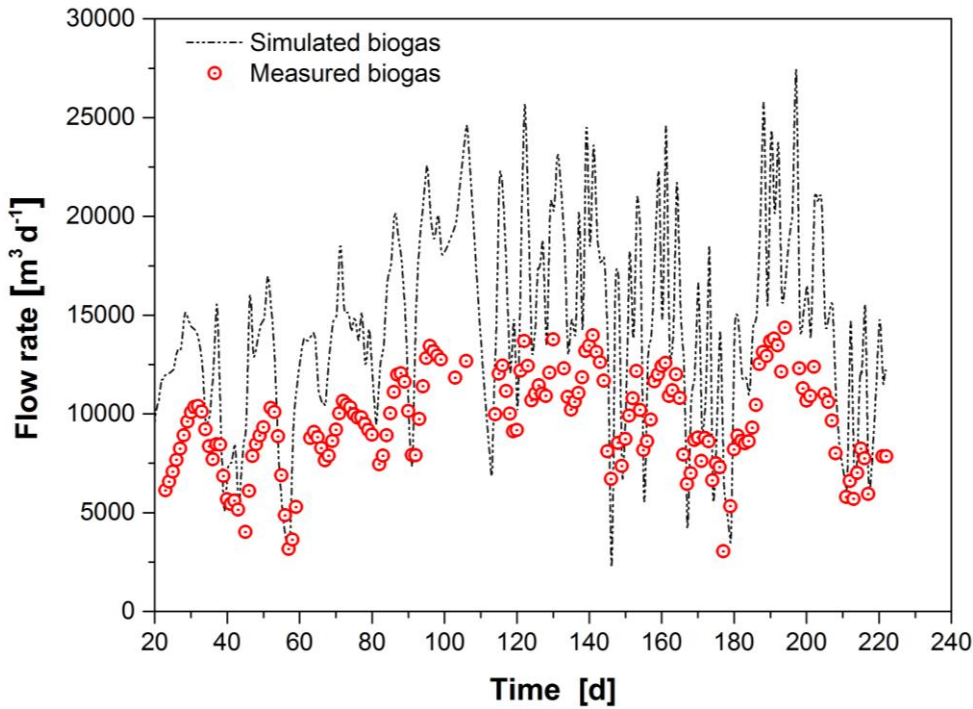
304
305 Figure 3. Averages of biogas and organic loading rate in 2012 and 2014

306 Ammonia inhibition is a key phenomenon affecting the dynamic of anaerobic digestion, especially
 307 the acetoclastic methanogenesis. A wide range of inhibiting ammonia concentrations has been
 308 reported in the literature, with the inhibitory TAN concentration that caused a 50% reduction in
 309 methane production rate ranging from 1.7 to 14 g/L (Chen et al. 2008). The inhibitory effect is due
 310 to free ammonia rather than ion ammonium: in the original ADM1 implementation, the 50%
 311 inhibitory concentration for the free ammonia is recommended at 0.0018 M, (i.e., 25 mg/L N-NH₃).
 312 In this study, the TAN concentration in the vinasse was, on average, 0.15 and 0.19 g/L in 2012 and
 313 2014, respectively, which at an experimental average pH of 7.5 and at 37° C, corresponds to a free
 314 ammonia concentration of 5.7 and 7.3 mg/L N-NH₃. Considering these values, it can be concluded
 315 that ammonia inhibition plays a minor role in the dynamics of the system. Furthermore, we show in
 316 Figure 3 a good correlation between the average organic loading and the biogas flow rate, as should
 317 be expected in a non-inhibited system.

318 Initial simulations, kinetic fractionation and parameter estimation

319 Initial dynamic simulations were performed to evaluate deviations between simulated and measured
 320 biogas, which are graphically evident in Figure 4. The default value for k_{hyd} and the assumed value
 321 for f_d are presented in Table 6. Both values were reduced after parameter estimation based on biogas
 322 yield showing great sensitivity. This study confirms that default ADM1 values of 10 d⁻¹ for
 323 hydrolysis constants are high as suggested in (Lübken et al. 2007, Vavilin et al. 2008).The

324 degradability f_d of 50% estimated is consistent with the characteristics of SV, which is composed by
 325 easily degradable organic material, mostly in the form of acetate and reducing sugars. In addition,
 326 as shown in Poggio et al. (2016) k_{hyd} and f_d are correlated parameters, which leads to increased
 327 uncertainty as observed in k_{hyd} . However, their correlation can offset possible adjustments between
 328 both parameters (Jensen et al. 2011).



329
 330 Figure 4. Initial dynamic simulations and results for measured biogas (markers) and simulated
 331 biogas (line).

332 Table 6. Results of model parameter estimation including initial values and standard errors.

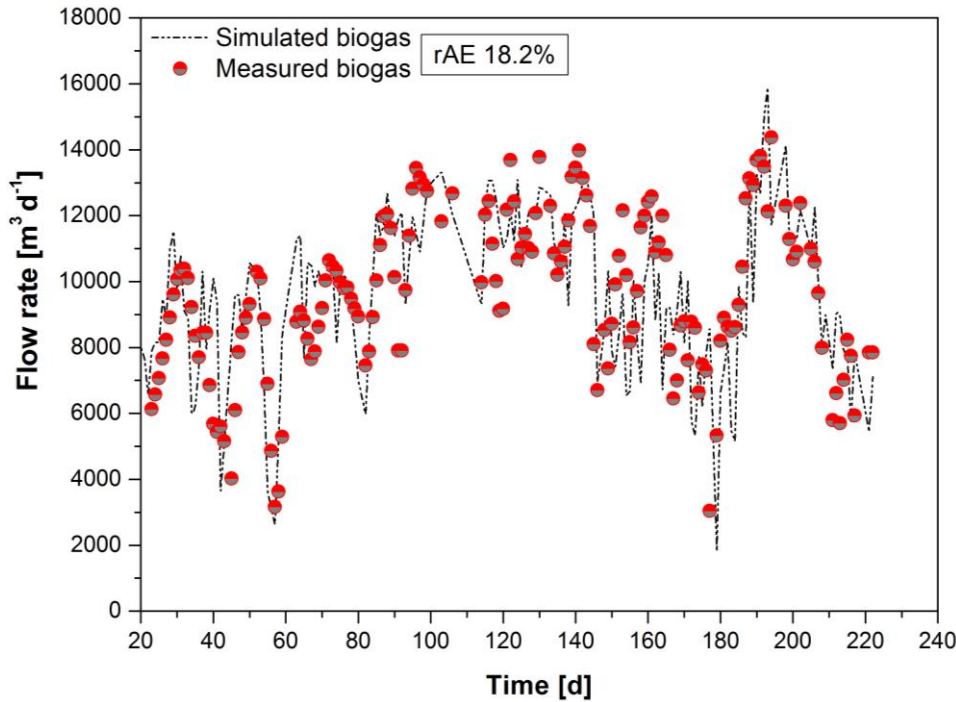
Parameters	Initial values	Estimated	Standard errors (%)
f_d	0.70 *	0.50	2.7
k_{hyd}	10 ^a	0.66	18.4

333 ^a ADM1 STR *assumed value

334 Direct validation

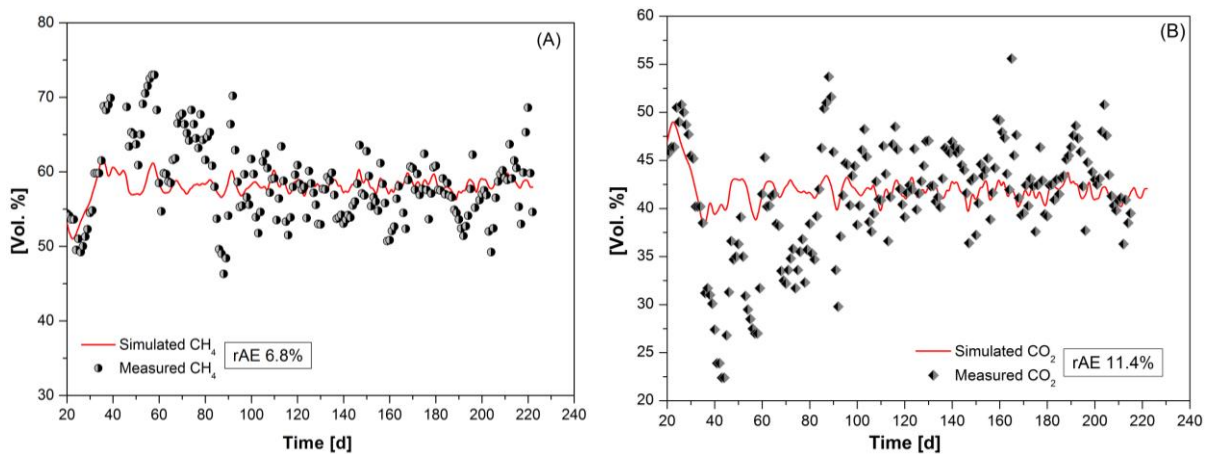
335 The simulations in Figure 5 indicate that, after parameter estimation of f_d and k_{hyd} , there is a good fit
 336 between simulated and measured biogas. The biogas prediction was assessed as medium, regarding
 337 18.2% of rAE. However, possible discrepancies between measurements and simulation results may
 338 be attributed to the ADM1 gas/liquid transfer coefficients for all gases, which in fact differ from
 339 reality (Ramirez et al. 2009b).

340



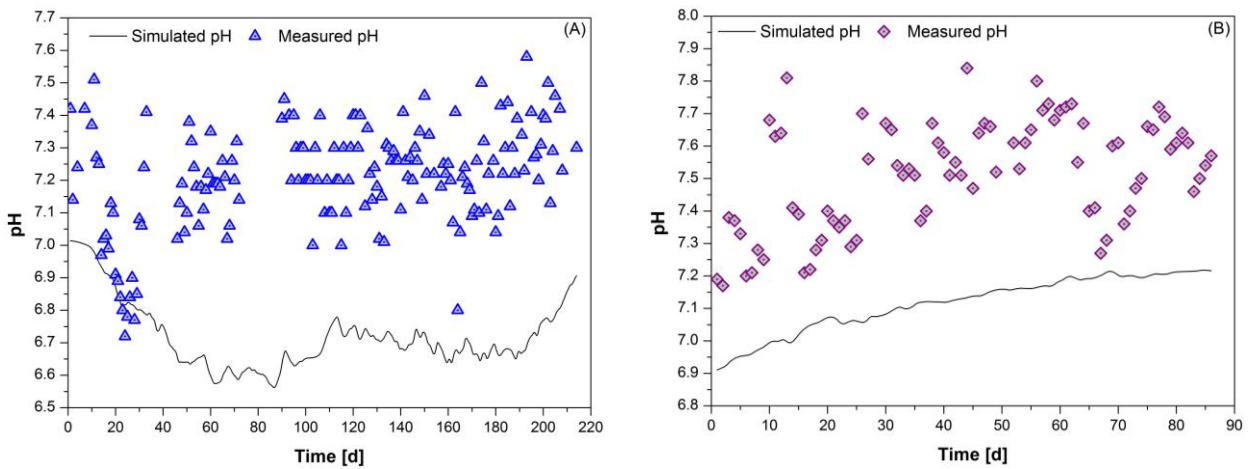
342
343 Figure 5. rAE for simulated results (line) and measured data (markers) for biogas production in
344 2012 – direct validation.

345 The deviations between simulated and measured outputs of methane and carbon dioxide levels after
346 the parameter estimation of f_d and k_{hyd} were also evaluated. The results are shown in Figure 6 (A)
347 and 6 (B), respectively. A good fit was achieved both for methane and carbon dioxide, which is an
348 indicator for a realistic substrate characterization (Lübken et al. 2007). These predictions were
349 assessed as high accuracy quantitative for methane with 6.8% of rAE and medium for carbon
350 dioxide with 11.4 % of rAE.



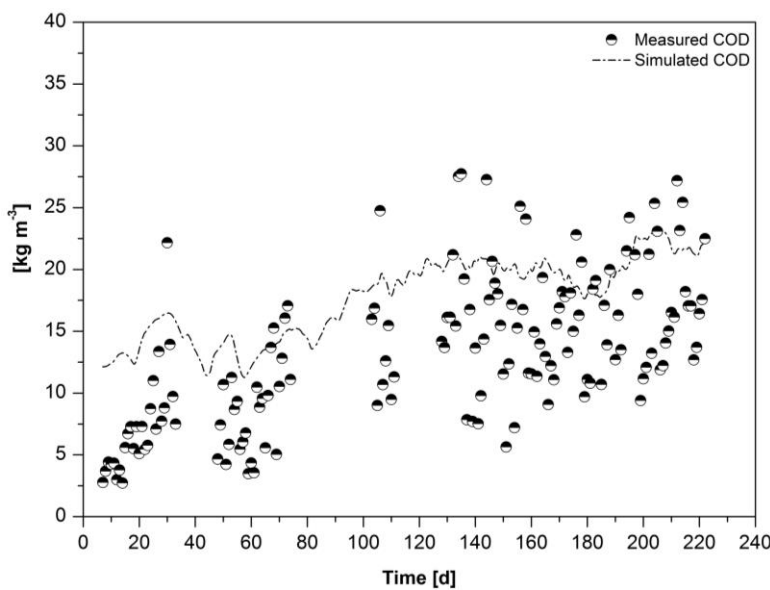
351
352 Figure 6. rAE for simulated results (line) and measured data (markers) for methane (A) and carbon
353 dioxide (B) – direct validation.

354 The difference between the concentrations of anions and cations calculated in the feeds predicts the
 355 pH in the system (Ramirez et al. 2009b). The simulations of pH variable, shown in Figure 7 (A) and
 356 6 (B), tend to underestimate the pH in both periods. This lack of fit could be explained by possible
 357 inaccuracies in the description of the charge balance of the substrate, with cations and anions
 358 loading, being calculated only during the dates presented in Table 5; apart from these dates yearly
 359 average values were used. Only between day 20 and 30 for the period of 2012 the model was able
 360 to improve the fit.



361
 362 Figure 7. Simulated results (line) and measured data (markers) for pH in both periods under study:
 363 2012 (A) and 2014 (B).

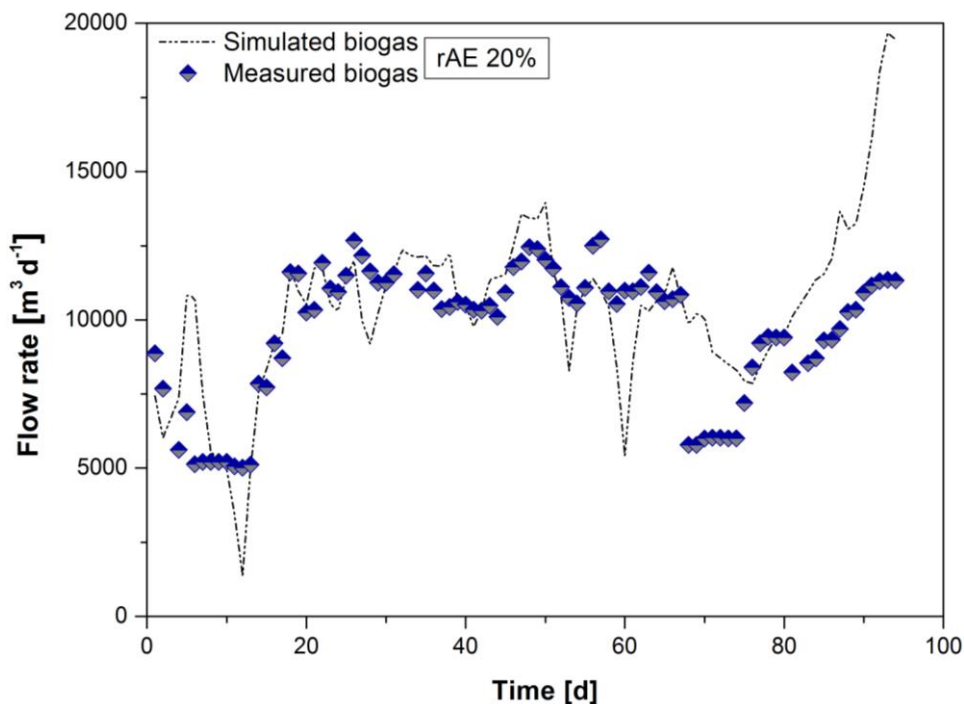
364 The model tends to over predict the COD concentrations (Figure 8), although, the trend is
 365 qualitatively followed by an increase in the COD concentrations.



366
 367 Figure 8. Simulated results (line) and measured data (markers) for COD concentrations in 2012.

368 **Cross validation**

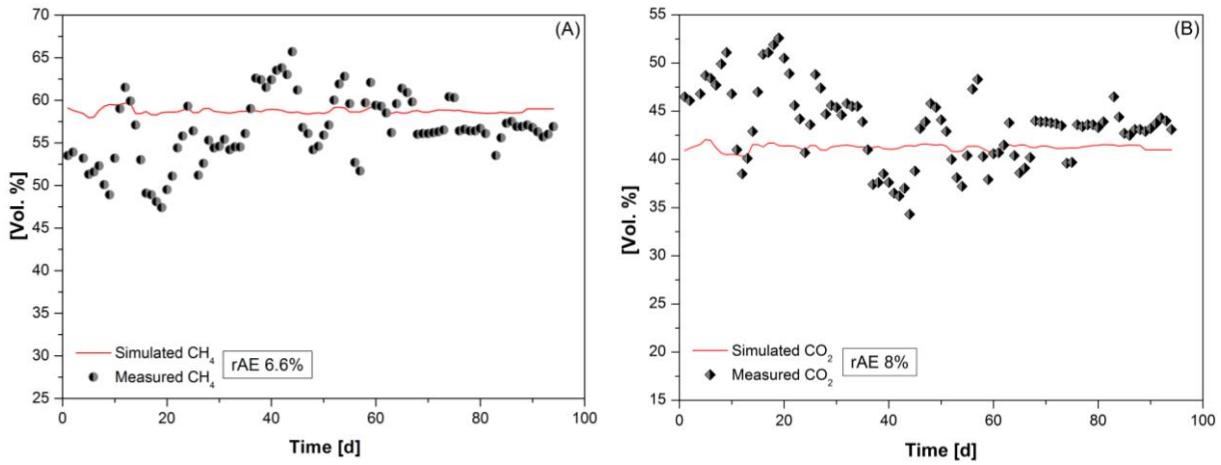
369 The cross validation procedure was implemented to check whether the model gives a reliable
 370 picture of the quality of the prediction on a second dataset after parameter estimation. To this end,
 371 the same values for the estimated parameters were kept in the cross validation. The Cigar operation
 372 summed up 96 days in 2014 under the same setup previously described in 2012.
 373 As presented in Figure 9, samples of biogas in 2014 are fewer than in 2012 but do so clearly and
 374 visibly a good fit between measured and simulated biogas. At the same time, the quality of biogas
 375 prediction was classified as medium accuracy showing a higher error (rAE 20%) resulting in a
 376 lower quality of prediction. This suggests that an increased solids concentration in the vinasse in
 377 2014, as observed in Table 3, compared to 2012 may be affecting the estimated hydrolysis constants
 378 of 0.66 d^{-1} , which are sensitive to solids concentration (Köch et al. 2010).



379 Figure 9. rAE for simulated results (line) and measured data (markers) for biogas production in
 380 2014 – cross validation.
 381

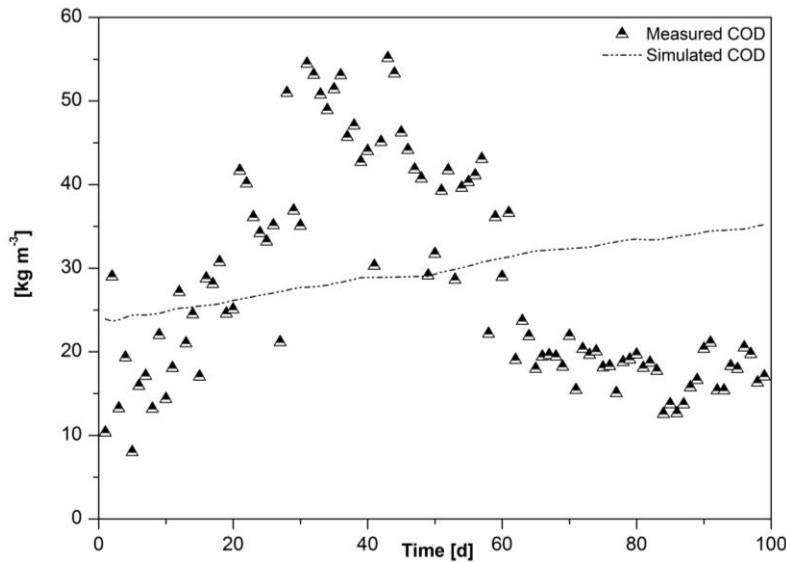
382 The rAE of 6.6% and 8% for methane and carbon dioxide, respectively, confirm the well fitted
 383 visual impression of the plots in Figure 10 (A) and 10 (B). The error for methane in the cross
 384 validation (rAE 6.6%) was quite similar to direct validation (rAE 6.8%), and validates the value of
 385 the estimate degradation extent (f_d) describing the degradable ThOD fraction of substrate that is
 386 converted to methane. Again, followed by a lower error (rAE 8%) for carbon dioxide in the cross

387 validation (Figure 10 (B)), a good prediction of biogas composition showed an evidence of realistic
388 substrate characterization (Lübken et al. 2007).



389
390 Figure 10. rAE for simulated results (line) and measured data (markers) for (A) methane and (B)
391 carbon dioxide – cross validation.

392 As noted in Figure 11, there were significant fluctuations in the measured COD concentrations that
393 could not be explained by the model in 2014. This result suggests that possibly, some parameters
394 not calibrated in this study are reflecting an inconsistency between simulated and measured COD
395 concentrations.



396
397 Figure 11. Simulated results (line) and measured data (markers) for COD concentrations in 2014.

398

399

400

401

402 CONCLUSIONS

403 Motivated by practical and industrial application of ADM1, for both different reactors types and
404 substrates, we have demonstrated in a clear procedure the implementation of ADM1 to specific
405 large-scale reactor for anaerobic digestion of sugarcane vinasse. The substrate characterization for
406 ADM1 in terms of its biochemical make-up (i.e., carbohydrates, proteins, and lipids), based on the
407 food industry standards were found to be valid when applied to describe sugarcane vinasse. The
408 quality of the predictions supported by the uncertainty of the estimation of the parameters, as given
409 by their calculated standard errors, provides a trustworthy assessment of the model performance on
410 future data. However, the lack of data to provide ADM1 charge balance inputs to cover all dynamic
411 feed streams resulted in poor pH simulations.

412 Therefore, taking into account the scale of the reactor presented here and the complexity of ADM1,
413 a practical industrial application to model a large-scale anaerobic digester under dynamic feed
414 streams, is a useful tool to predict the biogas yields and its composition.

415 ACKNOWLEDGMENTS

416 We thank Usina Ester and Omnis Biotecnologia for providing access to the operational data. The
417 work was supported by the Brazilian federal agency for support and evaluation of graduate
418 education – CAPES (process number 99999.010883/2014-02). We gratefully acknowledge
419 Professor Damien Batstone for providing the original ADM1 implementation in Aquasim.

420 REFERENCES

- 421 Arnell, M., Astals, S., Åmand, L., Batstone, D. J., Jensen, P. D. & Jeppsson, U. 2016 Modelling
422 anaerobic co-digestion in Benchmark Simulation Model No. 2: Parameter estimation, substrate
423 characterisation and plant-wide integration. *Water Research*, **98** (2), 138–146.
424 DOI:10.1016/j.watres.2016.03.070.
- 425 Angelidaki, I. & Sanders, W. 2004. Assessment of the anaerobic biodegradability of
426 macropollutants. *Reviews in Environmental Science & Biotechnol*, **3**, 117–129.
427 DOI:10.1007/s11157-004-2502-3.
- 428 APHA/AWWA/WEF 2012 *Standard Methods for the Examination of Water and Wastewater*, 22nd
429 edn. American Public Health Association/American Water Works Association/Water
430 Environment Federation, Washington, DC, USA.

431

432

- 433 Barrera, E. L., Spanjers, H., Solon, K., Amerlinck, Y., Nopens, I. & Dewulf, J. 2015 Modeling the
434 anaerobic digestion of cane-molasses vinasse: Extension of the Anaerobic Digestion Model
435 No. 1 (ADM1) with sulfate reduction for a very high strength and sulfate rich wastewater.
436 *Water Research*, **71** (1), 42–54. DOI:10.1016/j.watres.2014.12.026.
- 437 Batstone, D. J. & Keller, J. 2003 Industrial applications of the IWA anaerobic digestion model No.1
438 (ADM1). *Water Science and Technology*, **47** (12), 199–206.
- 439 Batstone, D. J., Keller, J. & Steyer, J. P. 2006 A review of ADM1 extensions, applications, and
440 analysis: 2002-2005. *Water Science and Technology*, **54** (4), 1–10. DOI:10.2166/wst.2006.520.
- 441 Batstone, D. J. & Steyer, J. P. 2007 Use of modelling to evaluate best control practice for winery-
442 type wastewaters. *Water Science and Technology*, **56** (2), 147–152.
443 DOI:10.2166/wst.2007.483.
- 444 Batstone, D. J., Tait, S. & Starrenburg, D. 2009 Estimation of hydrolysis parameters in full-scale
445 anaerobic digesters. *Biotechnology and Bioengineering*, **102** (5), 1513–1520.
446 DOI:10.1002/bit.22163.
- 447 Batstone, D. J., Balthes C. & K. Barr 2010 Model assisted startup of anaerobic digesters fed with
448 thermally hydrolysed activated sludge. *Water Science and Technology*, **62** (7), 1661 - 1666.
449 DOI:10.2166/wst.2010.487.
- 450 Batstone, D. J., Keller, J., Angelidaki, I., Kalyuzhnyi, S., Pavlostathis, S., Rozzi, A., Sanders, W.
451 T., Siegrist, H. & Vavilin, V. 2002 The IWA Anaerobic Digestion Model No 1(ADM1). *Water
452 Science and Technology*, **45** (1), 65–73. DOI:10.2166/wst.2008.678.
- 453 Bligh, E. G. & Dyer, W. J. 1959 *Canadian Journal of Biochemistry and Physiology*, **37** (8), 911–
454 917.
- 455 Chen, Y., Cheng, J. J. & Creamer, K. S. 2008 Inhibition of anaerobic digestion process: A review.
456 *Bioresource Technology* **99** (10), 4044-4064. DOI:10.1016/j.biortech.2007.01.057
- 457 Donoso-Bravo, A., Mailier, J., Martin, C., Rodríguez, J., Aceves-Lara, C. A. & Wouwer A. V. 2011
458 Model selection, identification and validation in anaerobic digestion: A review. *Water
459 Research*, **45** (17), 5347–5364. DOI:10.1016/j.watres.2011.08.059.
- 460 Flores-Alsina, X., Kimberly, S., Mbamba, C. K., Tait, S., Gernaey, K. V., Jeppsson, U. & Batstone,
461 D. J. (2016) Modelling phosphorus (P), sulfur (S) and iron (Fe) interactions for dynamic
462 simulations of anaerobic digestion processes. *Water Research*, **95**, 370-382.
463 DOI:10.1016/j.watres.2016.03.012.
- 464 GAIN (Global Agricultural Information Network). Brazil Sugar Annual (2017)
465 <[https://gain.fas.usda.gov/Recent%20GAIN%20Publications/Sugar%20Annual_Sao%20Paulo
466 %20ATO_Brazil_4-19-2017.pdf](https://gain.fas.usda.gov/Recent%20GAIN%20Publications/Sugar%20Annual_Sao%20Paulo%20ATO_Brazil_4-19-2017.pdf)> (accessed 7 May 2017).
- 467 Heertjes, P. M. & Kuijvenhoven, L. J. 1982 Fluid flow pattern in upflow reactors for anaerobic
468 treatment of beet sugar factory wastewater. *Biotechnology and Bioengineering*, **XXIV**, 443–
469 459.
- 470 Jensen, P. D., Ge, H. & Batstone, D. J. 2011 Assessing the role of biochemical methane potential
471 tests in determining anaerobic degradability rate and extent. *Water Science and Technology*, **64**
472 (4), 880–886. DOI:10.2166/wst.2011.662.
- 473 Kazadi Mbamba C., Flores-Alsina X., Batstone, D. J. & Tait, S. 2016 Validation of a plant-wide
474 phosphorus modelling approach with minerals precipitation in a full-scale WWTP. *Water
475 Research*, **100**, 169–183. DOI:10.1016/j.watres.2016.05.003.
- 476 Köch, K., Lübken, M., Gehring, T., Wichern, M. & Horn, H. 2010 Biogas from grass silage -

- 477 Measurements and modeling with ADM1. *Bioresource Technology*, **101** (21), 8158–8165.
478 DOI:10.1016/j.biortech.2010.06.009.
- 479 Lane, J. & Eynon, L. 1923 Volumetric determination of reducing sugars by means of Fehling's
480 solution with methylene blue as indicator. *Journal of the Society of Chemical Industry*, XXV,
481 143-149.
- 482 Leite, A. F., Janke, L., Harms, H., Zang, J. W., Fonseca-Zang, W. A., Stinner, W. & Nikolausz, M.
483 2015 Assessment of the Variations in Characteristics and Methane Potential of Major Waste
484 Products from the Brazilian Bioethanol Industry along an Operating Season. *Energy and*
485 *Fuels*, **29** (7), 4022–4029. DOI:10.1021/ef502807s.
- 486 Lübken, M., Wichern, M., Schlattmann, M., Gronauer, A. & Horn, H. 2007 Modelling the energy
487 balance of an anaerobic digester fed with cattle manure and renewable energy crops. *Water*
488 *Research*, **41** (18), 4085–4096. DOI:10.1016/j.watres.2007.05.061.
- 489 Mariotti, F., Tomé, D. & Mirand, P. P. Converting Nitrogen into Protein - Beyond 6.25 and Jones'
490 Factors. *Critical Reviews in Food Science and Nutrition*, **48** (2), 177-184,
491 DOI:10.1080/10408390701279749.
- 492 Mata-Alvarez, J., Dosta, J., Macé, S. & Astals, S. 2011 Codigestion of solid wastes: A review of its
493 uses and perspectives including modeling. *Critical Reviews in Biotechnology*, **31** (2), 99–111.
494 DOI: 10.3109/07388551.2010.525496.
- 495 Moraes, B. S., Zaiat, M. & Bonomi, A. 2015 Anaerobic digestion of vinasse from sugarcane ethanol
496 production in Brazil: Challenges and perspectives. *Renewable and Sustainable Energy*
497 *Reviews*, **44**, 888–903. DOI:10.1016/j.rser.2015.01.023.
- 498 Nopens, I., Batstone, D. J., Copp, J. B., Jeppsson, U., Volcke, E., Alex, J., & Vanrolleghem, P. A.
499 2009 An ASM/ADM model interface for dynamic plant-wide simulation. *Water Research*, **43**
500 (7), 1913–1923. DOI:10.1016/j.watres.2009.01.012.
- 501 Peña, M. R., Mara, D. D. & Avella, G. P. 2006 Dispersion and treatment performance analysis of
502 an UASB reactor under different hydraulic loading rates. *Water Research*, **40**, 445–452.
503 DOI:10.1016/j.watres.2005.11.021.
- 504 Poggio, D., Walker M., Nimmo, W., Ma, L. & Pourkashanian, M. 2016 Modelling the anaerobic
505 digestion of solid organic waste - Substrate characterisation method for ADM1 using a
506 combined biochemical and kinetic parameter estimation approach. *Waste Management*, **53**,
507 40–54. DOI:10.1016/j.wasman.2016.04.024.
- 508 Pratt, S., Liew, D., Batstone, D. J., Werker, A. G., Morgan-Sagastume, F. & Lant, P. A. 2012
509 Inhibition by fatty acids during fermentation of pre-treated waste activated sludge. *Journal of*
510 *Biotechnology*, **159** (1–2), 38-43. DOI:10.1016/j.jbiotec.2012.02.001.
- 511 Ramirez, I., Mottet, A., Carrère, H., Déléris, S., Vedrenne, F. & Steyer, J. P. 2009a Modified
512 ADM1 disintegration/hydrolysis structures for modeling batch thermophilic anaerobic
513 digestion of thermally pretreated waste activated sludge. *Water Research*, **43** (14), 3479–3492.
514 DOI: 10.1016/j.watres.2009.05.023.
- 515 Ramirez, I., Volcke, E. I. P., Rajinikanth, R. & Steyer, J.P. 2009b Modeling microbial diversity in
516 anaerobic digestion through an extended ADM1 model. *Water Research*, **43** (11), 2787–800.
517 DOI: 10.1016/j.watres.2009.03.034.
- 518 Reichert, P. 1998 Computer Program for the Identification and Simulation of Aquatic Systems
519 (AQUASIM), Swiss Federal Institute for Environmental Science and Technology, Dübendorf,
520 Switzerland.

- 521 Rosén, C. & Jeppsson, U. 2006 Aspects on ADM1 Implementation within the BSM2 Framework.
522 Department of Industrial Electrical Engineering and Automation, Lund University, Lund,
523 Sweden.
- 524 Solon, K., Flores-Alsina, X., Kazadi-Mbamba, C., Volcke, E.I.P., Tait, S., Batstone, D. J., Gernaey,
525 K.V. & Jeppsson, U. 2015 Effects of ion strength and ion pairing on (plant-wide) modelling of
526 anaerobic digestion processes. *Water Research*, **70**, 235-245.
527 DOI:10.1016/j.watres.2014.11.035.
- 528 Solon, K. 2017 Extending Wastewater Treatment Process Models for Phosphorus Removal and
529 Recovery - A Framework for Plant-Wide Modelling of Phosphorus, Sulfur and Iron. PhD
530 Thesis, Division of Industrial Electrical Engineering and Automation, Faculty of Engineering,
531 Lund University, Sweden.
- 532 Vavilin, V. A., Fernandez, B., Palatsi, J. & Flotats, X. 2008 Hydrolysis kinetics in anaerobic
533 degradation of particulate organic material: An overview. *Waste Management*, **28** (6), 939–
534 951. DOI:10.1016/j.wasman.2007.03.028.
- 535 Wett, B., Takács, I., Batstone, D. J., Wilson, C. & Murthy, S. 2014 Anaerobic model for high-
536 solids or high-temperature digestion—additional pathway of acetate oxidation. *Water Science
537 and Technology*, **69** (8) 1634-1640. DOI:10.2166/wst.2014.047.
- 538 Wilson, C. A., Novak, J., Takacs, I., Wett, B., & Murthy, S. 2012 The kinetics of process dependent
539 ammonia inhibition of methanogenesis from acetic acid. *Water Research*, **46** (19), 6247-6256.
540 DOI:10.1016/j.watres.2012.08.028
- 541
- 542
- 543
- 544
- 545
- 546
- 547
- 548
- 549